Inorganic Chemistry

Article

pubs.acs.org/IC

Trialkylphosphine-Stabilized Copper(I) Gallium(III) Phenylchalcogenolate Complexes: Crystal Structures and Generation of Ternary Semiconductors by Thermolysis

Oliver Kluge and Harald Krautscheid*

Institut für Anorganische Chemie, Universität Leipzig, Johannisallee 29, 04103 Leipzig, Germany

Supporting Information

ABSTRACT: A series of organometallic trialkylphosphine-stabilized copper gallium phenylchalcogenolate complexes $[(R_3P)_mCu_nMe_{2-x}Ga(EPh)_{n+x+1}]$ (R = Me, Et, ^{i}Pr, ^{t}Bu; E = S, Se, Te; x = 0, 1) has been prepared and structurally characterized by X-ray diffraction. From their molecular structures three groups of compounds can be distinguished: ionic compounds, ring systems, and cage structures. All these complexes contain one gallium atom bound to one or two methyl groups, whereas the number of copper atoms, and therefore the nuclearity of the complexes, is variable and depends mainly on size and amount of phosphine ligand used in synthesis. The Ga−E bonds are relatively rigid, in contrast to flexible Cu−E bonds. The lengths of the latter are controlled by the coordination number and steric influences. The Ga−E bond lengths depend systematically on the number of methyl groups bound to the gallium atom, with somewhat shorter bonds in monomethyl compounds compared to dimethyl compounds. Quantum chemical computations reproduce this trend and show furthermore that the rotation of one phenyl group around the Ga−E bond is a low energy process with two distinct minima, corresponding to two different conformations found experimentally. Mixtures of different types of chalcogen atoms on molecular scale are possible, and then ligand exchange reactions in solution lead to mixed site occupation. In thermogravimetric studies the complexes were converted into the ternary semiconductors $CuGaE_2$. The thermolysis reaction is completed at temperatures between 250 and 400 °C, typically with lower temperatures for the heavier chalcogens. Because of significant release of Me_3Ga during the thermolysis process, and especially in case of copper excess in the precursor complexes, binary copper chalcogenides are obtained as additional thermolysis products. Quaternary semiconductors can be obtained from mixed chalcogen precursors.

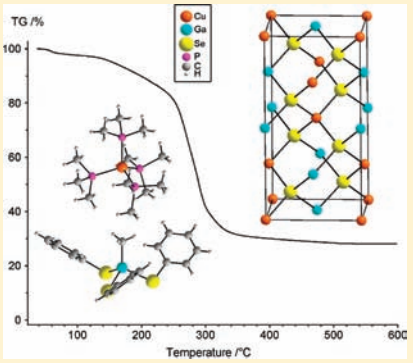

INTRODUCTION

The chalcopyrite type ternary semiconductors $Cu^IM^{III}E_2$ (M^{III} = Ga, In; E = S, Se) are suitable light absorbing materials for thin film solar cells.[1] In the industrial fabrication process, the thin films are usually deposited by coevaporation of the elements or by sulfurization/selenization of thin metal films.[1c] For the assessment of the results we present herein, it is important to know that the deposition involves at least one copper rich step in the case of the selenides,[2] and is performed with copper excess for the sulfides throughout.[3] The copper rich deposition results in larger grain sizes and furthermore improves the characteristics of the ternary semiconductor in view of its applicability in a thin film solar cell. The binary copper chalcogenides, which are obtained as additional phases, are easily removed from the thin film by chemical or electrochemical etching.

An alternative approach for the deposition of compound semiconductors is based on molecular precursors.[4] Besides some complex chalcogenolate anions, molecular chalcogenide and mixed chalcogenolate/chalcogenide complexes containing the desired elements Cu, Ga/In, and S/Se in a single molecule,[5] it was especially phosphine-stabilized chalcogenolate complexes of copper and group 13 metals that have attracted considerable attention in the past two decades,[6] since they can be used as single-source precursors for the thermolytic generation of the semiconductors $Cu^IM^{III}E_2$ (M^{III} = Ga, In; E = S, Se). These complexes may be modified by the types of group 13 and chalcogen atoms and with respect to the peripheral side groups at M^{III}, E, and P atoms. Although one can expect structural changes from these variations, most of the reported structures show a four-membered $Cu^IM^{III}E_2$ ring system as recurring complex core, which is usually stabilized by two Ph_3P ligands at the copper atom and two terminal chalcogenolate ligands at the group 13 atom. An early and repeatedly investigated example for such a complex is $[(Ph_3P)_2CuIn(SEt)_4]$.[6a]

It has been pointed out that the variations mentioned above will result in different behavior in the thermolysis process, but systematic studies dealing with this important point are scarce.[6c] Recent reports are more concerned with simplification, reproducibility, generalization, and upscaling of the synthetic procedures for the precursor complexes.[6l,m]

Although organometallic precursors are well established in processes for thin film deposition, such as MOCVD, and

Received: February 7, 2012
Published: June 7, 2012

dx.doi.org/10.1021/ic300278v | Inorg. Chem. 2012, 51, 6655−6666

despite the possibility of introducing organic residues at the group 13 atom instead of terminal chalcogenolate ligands claimed in the patent for the four-membered $Cu^{I}M^{III}E_2$ ring system,[6i] no organometallic single-source precursors for $Cu^{I}M^{III}E_2$ have been reported so far. As a first part of a systematic study concerning such organometallic precursors, a series of trialkylphosphine-stabilized copper gallium phenylchalcogenolate complexes is prepared and structurally characterized by single crystal X-ray diffraction, showing the structural consequences of introducing one or two methyl groups at the gallium atom, changing the type of chalcogen atom, for the first time including tellurium, and varying the steric demand of the phosphine ligand. In thermogravimetric experiments these complexes are converted into the respective semiconductor, the residue is characterized by X-ray powder diffraction. In addition, NMR spectroscopic and mass spectrometry data for the volatile thermolysis products allow a more detailed insight into the thermolysis reaction.

RESULTS AND DISCUSSION

1. Synthesis and Product Overview. From trialkylphosphine-stabilized copper phenylchalcogenolate complexes[7] $[(R_3P)_m(CuEPh)_n]$ (R = Me, Et, ^{i}Pr, ^{t}Bu; E = S, Se, Te) and dimethylgallium phenylchalcogenolates[8] $[(Me_2GaEPh)_n]$ the copper dimethylgallium phenylchalcogenolate complexes $[(R_3P)_mCu_nMe_2Ga(EPh)_{n+1}]$ (**1**, **2**, **6**–**8**) can be obtained in high yield by simply mixing the starting compounds in THF or toluene solution and subsequent crystallization of the products. The nearly quantitative yields indicate that the ternary complexes are more stable compared to the respective binary compounds. The copper dimethylgallium phenylchalcogenolate complexes can be converted into the corresponding monomethyl compounds $[(R_3P)_mCu_nMeGa(EPh)_{n+2}]$ (**3**–**5**, **9**–**18**) by addition of phenylchalcogenols and elimination of methane gas. For the heavier chalcogen atoms Se and Te it is useful to generate the free chalcogenol *in situ* from the silylated chalcogenol Me_3SiEPh and a protic compound, e.g., methanol, under elimination of Me_3SiOMe, since especially HTePh is unstable. Alternatively, the monomethyl compounds can be obtained directly from Me_3Ga and the copper complexes $[(R_3P)_m(CuEPh)_n]$ when 2 equiv of phenylchalcogenol is provided. The *in situ* generation of the copper complexes from R_3P, CuOAc, and Me_3SiEPh is also possible, but yields are lower. In general, it is necessary to use a protic solvent (MeOH) in order to complete the reaction of the second methyl group bound to the gallium atom with the free chalcogenol. The remaining methyl group is not sensitive to protolysis at room temperature and crystallization of the product is induced by interdiffusion with methanol. The main reactions are summarized in Scheme 1, and the formulas of the structurally characterized products are listed in Table 1. From the molecular structures the products can be assigned to three structural types, which will be discussed separately in the following sections.

Scheme 1. Summary of Reactions

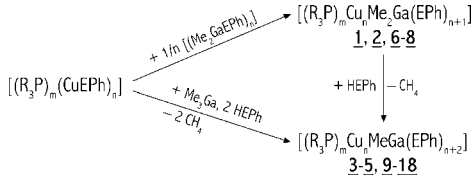

2. Ionic Compounds. *Crystal Structures.* By using 4 equiv of trimethylphosphine, Cu^+ ions can be shielded sterically, leading to the tetrahedral complex ion $[(Me_3P)_4Cu]^+$. Depending on the number of methyl groups bound to the gallium atom, the gallate ions $[Me_2Ga(EPh)_2]^-$ with E = S (**1**), Se (**2**) or $[MeGa(EPh)_3]^-$ with E = S (**3**), Se (**4**), Te (**5**) compensate the charge. Relevant crystallographic data for these five ionic compounds are listed in Table 2.

The dimethyl compounds **1** and **2** crystallize isostructurally in the monoclinic space group $P2_1/n$. The asymmetric unit contains both ions (Figure 1); therefore, no crystallographic symmetry is imposed within the ions. Nevertheless, the complex ion $[(Me_3P)_4Cu]^+$ shows approximately the point group symmetry T and the gallate ions $[Me_2Ga(EPh)_2]^-$ approximately C_2. The Cu–P bond lengths are in the typical range between 225.85(5) pm and 227.18(5) pm, and the P–Cu–P bond angles vary between 108.39(2)° and 110.76(4)°. The Ga–S bonds in **1** are 233.81(5) and 234.87(5) pm, and the Ga–Se bonds in **2** are 245.93(7) and 246.88(6) pm. Due to the larger C–Ga–C angles (118.9(1)° in **1** and 121.7(2)° in **2**) compared to the E–Ga–E angles (112.67(2)° in **1** and 112.17(3)° in **2**), the tetrahedral coordination of the gallium atom is distorted. This has to be expected from the extended VSEPR concept including dative bonds by Haaland.[9] It may be noted that the E–Ga–E angles are more than 10° larger than in the related binary compounds $[(Me_2GaEPh)_n]$ (E = S, Se),[8b] which can be explained by the stronger electrostatic repulsion of the partially negative chalcogen atoms in the present anions, and by the different coordination mode (terminal vs bridging).

The monomethyl compounds $[(Me_3P)_4Cu][MeGa(EPh)_3]$ with E = S (**3**), Se (**4**) again are isostructural and crystallize in the trigonal space group $P\bar{3}$. Both ions contain a crystallographic 3-fold axis passing through the copper and a phosphorus atom and through the gallium and the carbon atom, respectively. The resulting point group symmetry is C_3 for both ions, with the cation again near T. In contrast, the homologous tellurium compound **5** crystallizes monoclinic in $P2_1/c$, with no crystallographic symmetry in the ions. In **5** the 3-fold axis is lost because of a rotated phenyl group of a phenyltellurolate ligand (Figure 2). This may be due to packing effects, since compounds **3** and **4** cocrystallize with methanol, and the solvent filled pores increase from sulfur to selenium, whereas compound **5** does not contain any pores.

The structures of the cations in **3**, **4**, and **5** are very similar to those found in **1** and **2**. The Ga–E bond lengths in the anions of **3** (229.40(6) pm) and **4** (243.13(3) pm) are significantly shorter than in **1** and **2**, respectively. The bonds Ga1–Te1 and Ga1–Te3 in **5** are about 262 pm, and the bond Ga1–Te2 is somewhat longer (264.06(3) pm). As expected,[9] the angles C–Ga–E in **3** and **4** are more than 10° larger than the angles E–Ga–E. Due to the rotated phenyltellurolate ligand in **5** the angle C1–Ga1–Te2 is relatively small (109.19(8)°), but larger than the average Te–Ga–Te angle (106°).

Quantum Chemical Calculations. To further investigate some of the observed structural details, the gallate anion structures of **1**, **2**, **3**, and **4** were optimized with several quantum chemical methods. Minima were found in all cases in point group symmetries C_2 or C_3, respectively. Important geometrical parameters derived from optimizations are compared to (averaged) values from X-ray crystallography in Table 3. Whereas the reproduction of the Ga–E bond lengths

dx.doi.org/10.1021/ic300278v | Inorg. Chem. 2012, 51, 6655–6666

Table 1. Trialkylphosphine-Stabilized Copper(I) Gallium(III) Phenylchalcogenolate Complexes 1−18

	S	Se	Te
Me_3P	$[(Me_3P)_4Cu][Me_2Ga(SPh)_2]$ **1**	$[(Me_3P)_4Cu][Me_2Ga(SePh)_2]$ **2**	
	$[(Me_3P)_4Cu][MeGa(SPh)_3]$ **3**	$[(Me_3P)_4Cu][MeGa(SePh)_3]$ **4**	$[(Me_3P)_4Cu][MeGa(TePh)_3]$ **5**
	$[(Me_3P)_4Cu_6MeGa(SPh)_8]$ **14**	$[(Me_3P)_3Cu_4MeGa(SePh)_6]$ **15**	
Et_3P	$[(Et_3PCu)_2MeGa(SPh)_4]$ **9**	$[(Et_3P)_3Cu_4MeGa(SePh)_6]$ **16**	$[(Et_3P)_3Cu_4MeGa(TePh)_6]$ **18**
$Et_2{}^iPrP$	$[(Et_2{}^iPrPCu)_2MeGa(SPh)_4]$ **10**	$[(Et_2{}^iPrP)_3Cu_4MeGa(SePh)_6]$ **17**	
$^iPr_3P$	$[(^iPr_3PCu)_2Me_2Ga(SPh)_3]$ **6**		
	$[(^iPr_3PCu)_2MeGa(SPh)_4]$ **11**	$[(^iPr_3PCu)_2MeGa(SePh)_4]$ **12**	
	$[(^iPr_3PCu)_2MeGa(SPh)_3SePh]$ **13**		
$^tBu_3P$	$[(^tBu_3PCu)_2Me_2Ga(SPh)_3]$ **7**	$[(^tBu_3PCu)_2Me_2Ga(SePh)_3]$ **8**	

Table 2. Crystallographic Data for Ionic Compounds $[(Me_3P)_4Cu][Me_2Ga(EPh)_2]$ with E = S (1), Se (2) and $[(Me_3P)_4Cu][MeGa(EPh)_3]$ with E = S (3), Se (4), Te (5)

	1	**2**	**3**·$3CH_3OH$	**4**·$3CH_3OH$	**5**
chemical formula	$C_{26}H_{52}CuGaP_4S_2$	$C_{26}H_{52}CuGaP_4Se_2$	$C_{34}H_{66}CuGaO_3P_4S_3$	$C_{34}H_{66}CuGaO_3P_4Se_3$	$C_{31}H_{54}CuGaP_4Te_3$
fw [g mol^{-1}]	685.94	779.74	876.19	1016.89	1066.68
space group	$P2_1/n$ (No. 14)	$P2_1/n$ (No. 14)	$P\bar{3}$ (No. 147)	$P\bar{3}$ (No. 147)	$P2_1/c$ (No. 14)
a [Å]	13.8378(7)	13.8338(9)	13.1432(9)	13.317(1)	12.2974(9)
b [Å]	18.6786(8)	18.736(1)	13.1432(9)	13.317(1)	14.9911(6)
c [Å]	14.1980(7)	14.4290(8)	15.552(1)	15.802(2)	23.798(2)
α [deg]	90	90	90	90	90
β [deg]	90.624(4)	90.094(5)	90	90	91.811(5)
γ [deg]	90	90	120	120	90
V [Å^3]	3669.6(3)	3739.8(4)	2326.5(3)	2427.0(4)	4384.9(5)
Z	4	4	2	2	4
D_{calcd} [g cm^{-3}]	1.242	1.385	1.251	1.392	1.616
μ [Mo Kα, mm^{-1}]	1.615	3.420	1.336	3.402	3.219
R1 [$I > 2\sigma(I)$]	0.0239	0.0408	0.0287	0.0257	0.0222
wR2 [all data]	0.0546	0.0966	0.0634	0.0468	0.0377

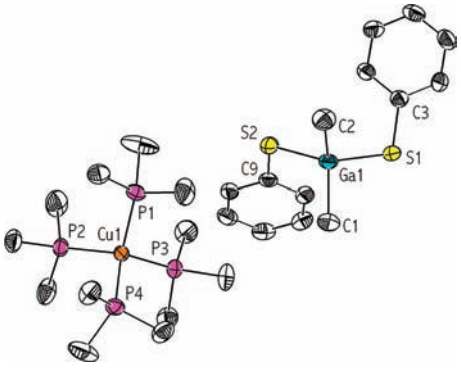

Figure 1. Molecular structure of $[(Me_3P)_4Cu][Me_2Ga(SPh)_2]$ (**1**). The homologous selenium compound **2** is isostructural. Hydrogen atoms are omitted for clarity, and thermal ellipsoids are drawn at 50% probability level.

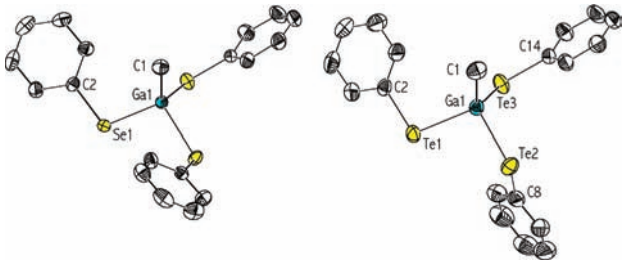

Figure 2. Gallate anions of $[(Me_3P)_4Cu][MeGa(SePh)_3]$ (**4**) and $[(Me_3P)_4Cu][MeGa(TePh)_3]$ (**5**). The homologous sulfur compound **3** is isostructural with **4**. Hydrogen atoms omitted, 50% probability ellipsoids.

is better on MP2 level, the overall geometry is better reproduced with DFT methods. On MP2 level of theory, the repulsive interaction between peripheral methyl and phenyl groups is obviously underestimated, leading to a contraction of the whole anion and Ga−E−C angles that are 10−15° smaller than those found experimentally. All calculated and experimental data agree in the Ga−E bond shortening of about 4 pm in the monomethyl systems compared to the dimethyl systems. This has to be expected from the concept of the dative bond.[9] From another viewpoint, this can also be explained by an improved delocalization of the charge that is transferred to the gallium atom, when a methyl group is substituted by a more electronegative phenylchalcogenolate ligand. For example, the Mulliken charge of the gallium atom according to DFT-(B3LYP) results is +0.48 in $[Me_2Ga(SPh)_2]^-$ and +0.74 in $[MeGa(SPh)_3]^-$. Consequently, the Ga−E bonds in the anions $[Ga(EPh)_4]^-$ (225.7 pm reported for E = S[10] and 240.2 pm for E = Se[11]) are even shorter.

To clarify the different observed conformations of anions, optimizations without symmetry restrictions were carried out on DFT (B3LYP and TPSSh) level of theory. One phenylchalcogenolate ligand was rotated manually in the starting structure, leading to new minima in C_1-symmetry with the main geometrical difference in the C−Ga−E−C torsion angles. These minima M2 are energetically slightly above the symmetrical minima M1. The respective transition states could also be located, and are only slightly above the minima, too. The B3LYP optimized anions are depicted in Figure 3. The TPSSh functional gives qualitatively the same potential energy

dx.doi.org/10.1021/ic300278v | Inorg. Chem. 2012, 51, 6655−6666

Table 3. Selected Bond Lengths [pm] and Angles [deg] for the Symmetrical Anions $[Me_2Ga(EPh)_2]^-$ and $[MeGa(EPh)_3]^-$ (E = S, Se) as Derived from DFT (B3LYP and TPSSh) and MP2 Optimizations in Comparison to Experimental Values from X-ray Crystallography

	$[Me_2Ga(SPh)_2]^-$				$[Me_2Ga(SePh)_2]^-$			
	B3LYP	TPSSh	MP2	exptl	B3LYP	TPSSh	MP2	exptl
Ga–E	238.9	237.0	234.1	234.3	252.0	249.7	246.0	246.4
Ga–C	200.5	200.2	198.0	198.4	200.7	200.3	198.0	198.0
E–Ga–E	112.5	113.0	107.9	112.7	112.3	113.0	106.9	112.2
C–Ga–C	120.6	120.8	121.6	118.9	120.4	120.8	121.1	121.7
Ga–E–C	107.9	107.8	98.6	108.0	104.3	104.3	94.6	105.8
	$[MeGa(SPh)_3]^-$				$[MeGa(SePh)_3]^-$			
	B3LYP	TPSSh	MP2	exptl	B3LYP	TPSSh	MP2	exptl
Ga–E	235.0	233.3	230.1	229.4	248.0	245.7	242.1	243.1
Ga–C	199.4	199.0	197.0	196.4	199.6	199.1	197.2	199.0
E–Ga–E	104.0	103.9	105.9	103.0	104.0	103.8	106.4	102.1
E–Ga–C	114.5	114.6	112.8	115.4	114.5	114.6	112.4	116.1
Ga–E–C	104.7	104.5	93.9	106.9	101.8	101.6	90.1	104.9

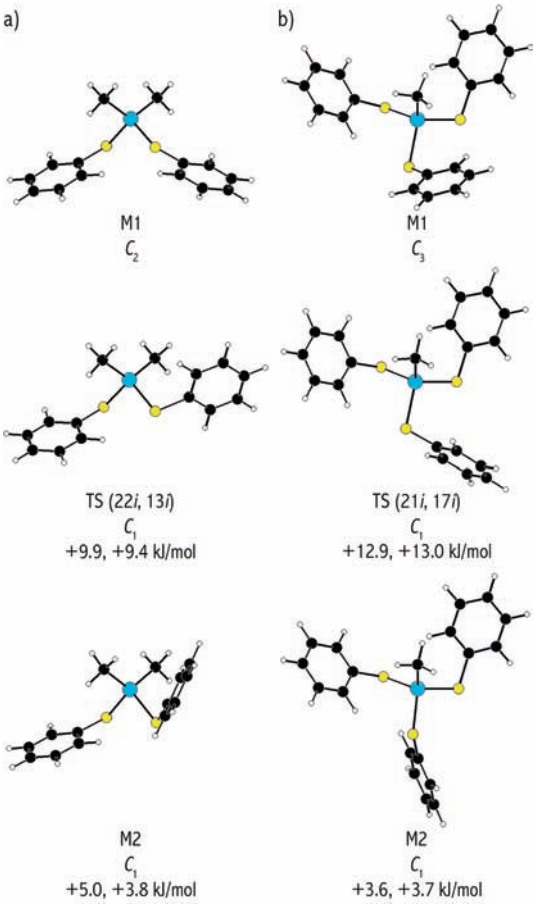

Figure 3. Gallate anions (a) $[Me_2Ga(EPh)_2]^-$ and (b) $[MeGa(EPh)_3]^-$ from DFT(B3LYP) optimizations. Together with the stationary point (M = minimum, TS = transition state) and the point group symmetry, imaginary frequencies and relative energies are given for E = S and Se, respectively.

surface, the relative energies of the minima change less than 1 kJ/mol, and the relative energies of the transition states increase systematically by 1–3 kJ/mol.

Regarding the small energetic difference between the minima, it seems reasonable that the observed conformational difference in **3** and **4** versus **5** is due to packing effects. Furthermore, the flat potential energy surface may contribute to the relatively low melting points (between 70 and 100 °C) of compounds **1**–**5**, since conformational flexibility is thought to be one key aspect for the design of ionic liquids, as is the size of anions.[12] Comparing the isostructural compounds **1** and **2** or **3** and **4**, the selenium compounds do melt at lower temperatures in both cases.

Thermolysis. In a typical experiment, a small amount (20–40 mg) of substance was heated with a heating rate of 10 K/min to 600 °C on a thermobalance, and beside the thermogravimetric (TG) curve, a differential scanning calorimetry (DSC) curve as well as ion current curves of selected fragments were detected simultaneously. As an example, the obtained data for **1** is shown in Figure 4.

After thermolysis, a high quality X-ray powder diffraction pattern of the residue was obtained and a quantitative phase analysis was performed by the Rietveld refinement method. For compound **1** all the obtained data are consistent with the following overall thermolysis reaction:

$$3[(Me_3P)_4Cu][Me_2Ga(SPh)_2] \xrightarrow{\Delta T} 12Me_3P + 2Me_3Ga + 3SPh_2 + CuGaS_2 + Cu_2S \quad (1)$$

As can be seen from the TG curve and its first derivative (DTG), the reaction proceeds in two steps. The first step corresponds to the complete loss of trimethylphosphine (mass change 43.4%, calcd 44.4%), and the respective ion current curve (m/z = 76 for Me_3P^+) runs through a maximum. In the second step SPh_2 (m/z = 186 for SPh_2^+, m/z = 78 for $C_6H_6^+$) can be detected, its boiling point of 296 °C fitting well with the onset temperature for the respective ion current curves. The maximum for the ion current curve with m/z = 15 (CH_3^+) at approximately 300 °C may be explained by the simultaneous loss of Me_3Ga. The overall mass change of 82.2% (calcd 82.8%) is complete at 346 °C (extrapolated from TG curve). According to the Rietveld phase analysis the residue consists of 56.8(1) wt. % $CuGaS_2$ and 43.2(8) % tetragonal Cu_2S.[13] In reasonable agreement (the error of such phase analysis has always to be expected in the range of few percents), 55.4% $CuGaS_2$ and 44.6% Cu_2S are to be expected from the reaction shown in eq 1.

The selenium homologue **2** obviously decomposes with a slightly different mechanism. Only one inflection is found in the

dx.doi.org/10.1021/ic300278v | *Inorg. Chem.* 2012, 51, 6655–6666

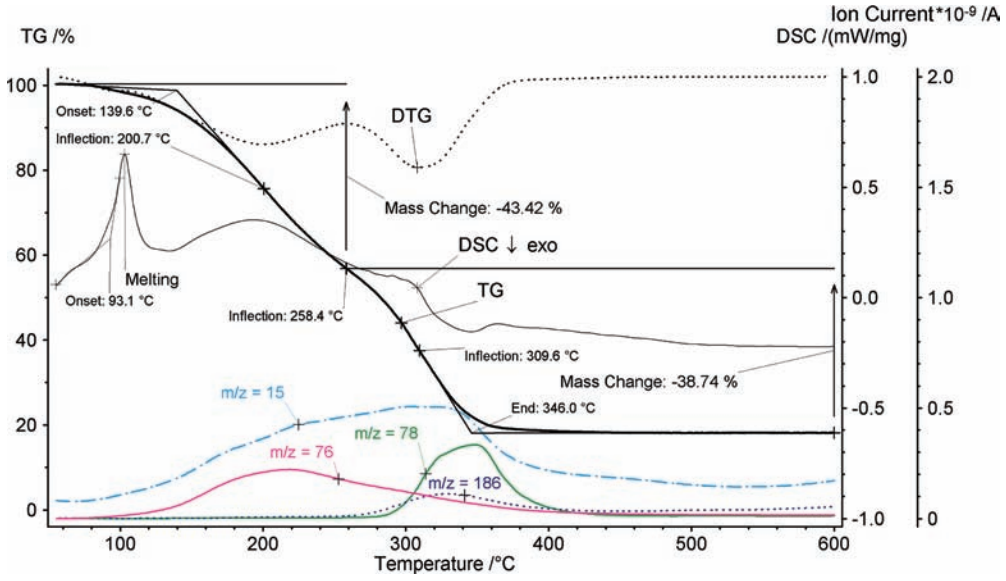

Figure 4. Thermolysis of compound **1**. The thermogravimetric curve (TG), its first derivative (DTG), the differential scanning calorimetry curve (DSC), and selected ion current curves (m/z = 186 multiplied by factor 100) are shown.

TG curve, so the thermolysis proceeds in a single step with a mass change of 76.2% (calcd 77.5% for the reaction analogous to **1**). The extrapolated end temperature (272 °C) is lower than for **1**, so the quantitative release of $SePh_2$, which has even a higher boiling point than SPh_2, is very unlikely. Instead we could detect MeSePh (m/z = 170 and 172) which may be an exchange product from $SePh_2$ and Me_3Ga, and has a sufficient low boiling point of 201 °C. To further confirm this observation, we collected the volatile thermolysis products from an additional experiment with a larger amount of substance in a cold trap, and separated them by their volatility into three fractions. The most volatile fraction contained mainly Me_3P, and the second fraction was a mixture of a low melting solid and a clear liquid. From multicore NMR spectral data,[14] the low melting solid was identified as the adduct Me_3Ga–PMe_3 (mp 56 °C)[15] and the liquid as MeSePh. The third fraction additionally contained $SePh_2$ and a small amount of Me_3PSe. However, the residue of the thermolysis reaction of **2**, similar to **1**, consists of 48.83(9) % $CuGaSe_2$ and 51.2(2) % cubic $Cu_{2-x}Se$.[16]

For the monomethyl compounds **3**–**5** the loss of Me_3Ga can be expected to be less than that for **1** and **2**, and the amount of ternary chalcogenide in the residue should be higher, respectively. As it turned out, the mass loss for these three compounds is between the calculated values for the release of the methyl groups as Me_3Ga or toluene, which can be a recombination product, when a radical mechanism is assumed for the cleavage of the Ga–C and E–C bonds. Therefore, it seems likely that both mechanisms concur. The quantity of the resulting ternary semiconductor critically depends on the maximum temperature of the thermolysis experiment, with higher temperatures resulting in higher proportions of $CuGaE_2$. Binary copper chalcogenides are observed as additional phases, and we assume that also amorphous binary gallium chalcogenides are formed, which form $CuGaE_2$ with $Cu_{2-x}E$ at higher temperatures in a solid state reaction. With a maximum temperature of 850 °C, a proportion of nearly 90% $CuGaS_2$ is found in the residue of **3**, according to Rietveld phase analysis. Table 4 summarizes some important results of the thermolysis experiments of the ionic compounds **1**–**5**; more detailed information including TG curves and Rietveld refinement plots are given in the Supporting Information (Figures S15–S19 and S30–S35).

Table 4. Results of Thermolysis Experiments for Compounds 1–5

	T_{max} [°C]	T_{end}[a] [°C]	$CuGaE_2$[b] [%]
1	600	346	56.8(1)
2	600	272	48.83(9)
3	600	350	68.9(2)
3	850	366	89.45(3)
4	600	309	79.40(5)
5	600	368	70.40(9)

[a]Completion of mass loss extrapolated from TG curve. [b]Proportion of ternary chalcogenide in the residue, standard deviations from Rietveld refinement are given in parentheses.

3. Ring Systems. *Crystal Structures.* With bulkier phosphine ligands we obtained the six-membered ring systems $[(R_3PCu)_2Me_2Ga(EPh)_3]$ with R = ^{i}Pr, E = S (**6**) and R = ^{t}Bu, E = S (**7**), Se (**8**). These three structures are shown in Figure 5, and relevant crystallographic data are listed in Table 5. With one phosphine ligand and two phenylchalcogenolate ligands, each copper atom is trigonal planar coordinated. The Me_2Ga unit completes the Cu_2GaE_3 ring system.

Although all three complexes crystallize in the same monoclinic space group type, they are not isostructural, since the placement of the rings in the unit cell and the conformations of the rings differ significantly. A quantitative conformation analysis according to Cremer and Pople shows that the conformation of **6** is nearly ideal twist boat, whereas **7** and **8** are between boat and twist boat, with different positions of the gallium atom in the ring.[17]

The Cu–E bond lengths have the usual values for 3-fold coordinated copper (Cu–S 224–229 pm; Cu–Se 237–244 pm), except the bonds Cu1–S1 (233.17(8) pm) and Cu2–S2 (235.68(9) pm) in **7**, which are relatively long as a result of steric strain. It is interesting that the elongation affects selectively these two bonds but not the respective Ga–S bonds, which are about 236 pm long in **6** as well as in **7**. Ga–Se

dx.doi.org/10.1021/ic300278v | Inorg. Chem. 2012, 51, 6655–6666

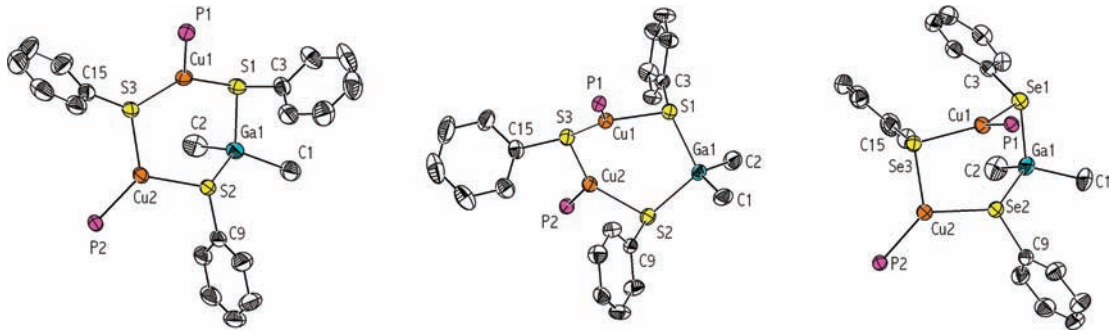

Figure 5. Molecular structures of $[(^{i}Pr_3PCu)_2Me_2Ga(SPh)_3]$ (**6**), $[(^{t}Bu_3PCu)_2Me_2Ga(SPh)_3]$ (**7**), and $[(^{t}Bu_3PCu)_2Me_2Ga(SePh)_3]$ (**8**). Hydrogen atoms and alkyl groups of phosphine ligands omitted, 50% probability ellipsoids.

Table 5. Crystallographic Data for Compounds $[(R_3PCu)_2Me_2Ga(SPh)_3]$ with R = ^{i}Pr (6), ^{t}Bu (7) and $[(^{t}Bu_3PCu)_2Me_2Ga(SePh)_3]$ (8)

	6	7	8
chemical formula	$C_{38}H_{63}Cu_2GaP_2S_3$	$C_{44}H_{75}Cu_2GaP_2S_3$	$C_{44}H_{75}Cu_2GaP_2Se_3$
fw [g mol^{-1}]	874.80	958.96	1099.66
space group	$P2_1/n$ (No. 14)	$P2_1/c$ (No. 14)	$P2_1/c$ (No. 14)
a [Å]	12.0245(6)	18.7165(9)	13.6272(7)
b [Å]	16.8548(6)	11.7912(7)	13.0077(5)
c [Å]	22.419(1)	23.011(1)	28.082(1)
α [deg]	90	90	90
β [deg]	103.327(4)	109.828(4)	97.114(4)
γ [deg]	90	90	90
V [Å^3]	4421.4(3)	4777.1(4)	4939.5(4)
Z	4	4	4
D_{calcd} [g cm^{-3}]	1.314	1.333	1.479
μ [Mo Kα, mm^{-1}]	1.796	1.669	3.698
R1 [$I > 2\sigma(I)$]	0.0388	0.0372	0.0269
wR2 [all data]	0.1057	0.0646	0.0613

Table 6. Crystallographic Data for Compounds $[(R_3PCu)_2MeGa(SPh)_4]$ with R_3P = Et_3P (9), $Et_2{}^{i}PrP$ (10), $^{i}Pr_3P$ (11), $[(^{i}Pr_3PCu)_2MeGa(SePh)_4]$ (12), and $[(^{i}Pr_3PCu)_2MeGa(SPh)_3SePh]$ (13)

	9	10	11	12	13
chemical formula	$C_{37}H_{53}Cu_2GaP_2S_4$	$C_{39}H_{57}Cu_2GaP_2S_4$	$C_{43}H_{65}Cu_2GaP_2S_4$	$C_{43}H_{65}Cu_2GaP_2Se_4$	$C_{43}H_{65}Cu_2GaP_2S_3Se$
fw [g mol^{-1}]	884.77	912.83	968.93	1156.53	1015.83
space group	$P2_1/n$ (No. 14)	$P2_1/c$ (No. 14)	$P2_1/c$ (No. 14)	$P2_1/c$ (No. 14)	$P2_1/c$ (No. 14)
a [Å]	17.0527(9)	11.6285(6)	12.2982(5)	12.3284(4)	12.1909(5)
b [Å]	12.6070(4)	39.204(2)	39.431(1)	40.095(2)	39.508(1)
c [Å]	20.238(1)	10.2233(5)	10.6803(4)	10.8926(4)	10.7364(4)
α [deg]	90	90	90	90	90
β [deg]	103.841(4)	109.528(4)	113.751(3)	113.723(3)	113.241(3)
γ [deg]	90	90	90	90	90
V [Å^3]	4224.6(3)	4392.6(4)	4740.5(3)	4929.3(3)	4751.5(3)
Z	4	4	4	4	4
D_{calcd} [g cm^{-3}]	1.391	1.380	1.358	1.558	1.420
μ [Mo Kα, mm^{-1}]	1.928	1.857	1.725	4.443	2.443
R1 [$I > 2\sigma(I)$]	0.0416	0.0543	0.0367	0.0323	0.0519
wR2 [all data]	0.1161	0.1518	0.1072	0.0742	0.1398

bond lengths in **8** are 248.51(4) pm and 251.83(4) pm. The most flexible parameter in the $Me_2Ga(EPh)_2^-$ unit contained in these rings is the rotation of a whole phenylchalcogenolate ligand around the Ga−E bond, what has been shown above to be a low energy process for the free ions. Whereas in **6** and **8** the $Me_2Ga(EPh)_2^-$ fragments are far from C_2-symmetry, in **7** this fragment is very similar to the C_2-symmetrical free ion in **1**. In general, C−Ga−C angles are around 120°, and the E−Ga−E angles (96° to 110°) are smaller.

If compound **6** is reacted with an additional equivalent of phenylthiol, one methyl group at the gallium atom is replaced by a phenylthiolate ligand, leading to the compound $[(^{i}Pr_3PCu)_2MeGa(SPh)_4]$ (**11**). From Me_3Ga and copper phenylchalcogenolate complexes this system is also accessible with the smaller phosphine ligands Et_3P and $Et_2{}^{i}PrP$ (compounds **9** and **10**), and substitution of SPh ligands with SePh ligands is also possible (compounds **12** and **13**). Relevant crystallographic data for compounds **9**−**13** are listed in Table 6.

dx.doi.org/10.1021/ic300278v | Inorg. Chem. 2012, 51, 6655−6666

The molecular structure of **9** is shown in Figure 6. The six membered ring system from **6** and **7** is maintained, but bridged

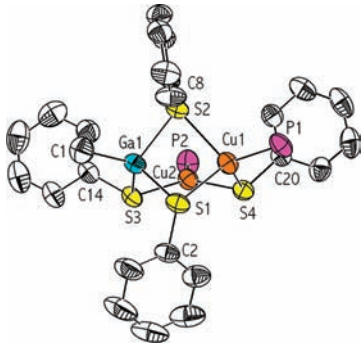

Figure 6. Molecular structure of $[(Et_3PCu)_2MeGa(SPh)_4]$ (**9**). Hydrogen atoms and alkyl groups of phosphine ligands omitted, 50% probability ellipsoids.

by the additional phenylthiolate ligand. This results in 4-fold coordination of Cu1, with a relatively long bond Cu1−S2 of 249.7(1) pm. Due to the increasing steric demand of the phosphine ligands this bond is further elongated to 260.6(1) pm in **10** and to 286.6(1) pm in **11** (Figure 7). In the same

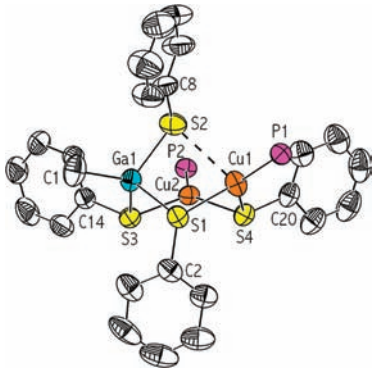

Figure 7. Molecular structure of $[(^iPr_3PCu)_2MeGa(SPh)_4]$ (**11**). Compounds **10**−**12** are isostructural. Hydrogen atoms and alkyl groups of phosphine ligands omitted, 50% probability ellipsoids.

series, the out of plane parameter d_{Cu1}(P1, S1, S4) decreases from 58.6 pm over 44.7 to 33.0 pm. The latter value is typical for a secondary Cu···S connection,[7b] so the steric influence of the phosphine ligands continuously changes the coordination sphere of Cu1 from tetrahedral to nearly trigonal planar. In contrast, the Ga−S bond lengths are not affected, being rigid with values between 230.11(9) pm to 232.3(1) pm. As expected,[9] that is significantly shorter than in the related dimethyl compounds **6** and **7**.

In compound **12**, the selenium homologue of **11**, the steric strain is diminished by the larger heavy atom core, but again the longest Cu−Se bond is Cu1−Se2 with 274.67(6) pm. The other Cu1−Se bonds are 257.40(6) and 242.89(6) pm, which are more typical values for 4-fold coordinated copper. The Cu2−Se bond lengths are typical for the 3-fold coordination; values are 242.68(6) and 236.66(5) pm. The Ga−Se bond lengths range from 243.65(6) to 245.66(6) pm, 3−8 pm shorter than in the dimethyl compound **8**.

Since **11** can be easily synthesized from **6**, and because of the fact that **11** and **12** are isostructural, it seemed interesting to synthesize the mixed sulfur/selenium compound $[(^iPr_3PCu)_2MeGa(SPh)_3SePh]$ (**13**) by reacting **6** with one equivalent phenylselenol. The yield was quantitative, but according to the structure refinement and in contrast to our expectations, the phenylselenolate ligand does not only occupy the bridging position, but shares all four possible positions with the three phenylthiolate ligands. Obviously, ligand exchange reactions take place in solution, what is further supported by the NMR spectra of these compounds showing the typical line broadening, especially for the *ortho* hydrogen atoms. The resulting molecular structure of **13** is shown in Figure 8.

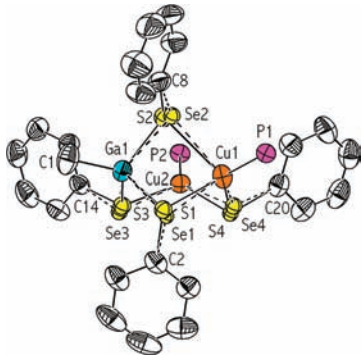

Figure 8. Molecular structure of $[(^iPr_3PCu)_2MeGa(SPh)_3SePh]$ (**13**). Hydrogen atoms and alkyl groups of phosphine ligands omitted, 50% probability ellipsoids.

The refinement of the occupancy factors shows that position E4 (E = S, Se) between the two copper centers is preferred by the selenium atom. This position is occupied by only 53.5(3)% sulfur atoms. The bridging position E2 is occupied by 67.8(3)% sulfur atoms, and E1 and E3 are occupied by 90.1(3)% and 88.1(3)% sulfur atoms, respectively. So the steric factor, reflecting that position E2 should be preferred by the selenium atom, does also have a significant influence.

Thermolysis. The compounds **6**−**9** and **11**−**13** were investigated in thermolysis experiments. From the results we obtained for the ionic compounds **1**−**5** it can be predicted that the residues will contain large proportions of binary copper chalcogenides, since **6**−**13** are more copper rich. As expected, this is especially the case for the dimethyl compounds **6**−**8**, where significant release of Me_3Ga during the thermolysis process leads to additional loss of gallium. Details of the thermolysis experiments, including an *in situ* X-ray powder diffraction study of the thermolysis of **12**, are given in the Supporting Information (Figures S20−S26, S36−S42, and S46), and the most important data are summarized in Table 7.

The extrapolated end temperatures are comparable to those of the ionic compounds, with lower end temperatures for selenium compounds. From the *in situ* X-ray powder diffraction patterns of the thermolysis of **12** (Figure S46) it is evident that crystalline $CuGaSe_2$ is formed at a temperature of approximately 270 °C, in good agreement with the end temperature extrapolated from the TG curve. The most interesting result is that the thermolysis of the mixed sulfur/selenium compound **13** yields a quaternary semiconductor of the approximate formula $CuGaS_{1.5}Se_{0.5}$, which was concluded from comparison of the cell constants of the pure ternary phases with those obtained for the quaternary phase in the residue of **13** from Rietveld refinement applying Vegard's rule. So the ratio between S and Se from the precursor complex is maintained

dx.doi.org/10.1021/ic300278v | *Inorg. Chem.* 2012, 51, 6655−6666

Table 7. Results of Thermolysis Experiments for Compounds 6−13 (T_{max} = 600 °C)

	T_{end}[a] [°C]	$CuGaE_2$[b] [%]
6	345	17.32(9)
7	339	32.9(2)
8	254	32.5(1)
9	347	61.0(1)
11	334	50.85(9)
12	275	39.40(5)
13	304	33.9(1)

[a]Completion of mass loss extrapolated from TG curve. [b]Proportion of ternary chalcogenide in the residue, standard deviations from Rietveld refinement are given in parentheses.

in the semiconductor; that means that mixing different types of chalcogen atoms on the molecular scale results in a mixed solid state chalcogenide. This provides an important opportunity, regarding the adjustment of the band gap of the resulting semiconductor.

4. Cage Structures. *Crystal Structures.* With less than 1 equiv of relatively small trialkylphosphine ligands, a third group of structures was obtained. These complexes are more copper rich than the ring systems and are all monomethyl gallium compounds. In contrast to the colorless compounds discussed above, the color of these complexes is yellow to orange. Depending on the type of chalcogen atom, two different structures are observed. The first type is represented by the sulfur compound $[(Me_3P)_4Cu_6MeGa(SPh)_8]$ (**14**, Figure 9),

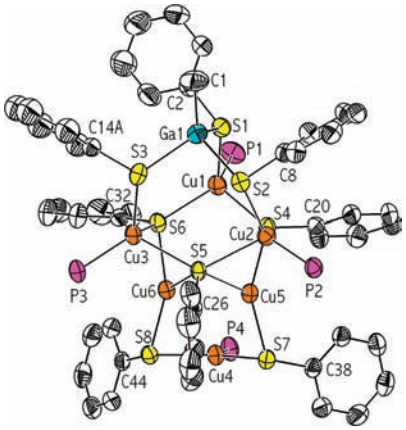

Figure 9. Molecular structure of $[(Me_3P)_4Cu_6MeGa(SPh)_8]$ (**14**). Hydrogen atoms and alkyl groups of phosphine ligands omitted, 50% probability ellipsoids.

and the second type is of the general formula $[(R_3P)_3Cu_4MeGa(EPh)_6]$ with E = Se and $R_3P = Me_3P$ (**15**), Et_3P (**16**), $Et_2{}^iPrP$ (**17**) and E = Te and $R_3P = Et_3P$ (**18**). Both structural types contain a $MeGa(EPh)_3^-$ group, but differ in the copper containing fragment, which is $(Me_3P)_4Cu_6(SPh)_5^+$ or $(R_3P)_3Cu_4(EPh)_3^+$, respectively. Relevant crystallographic data for these five cage structure compounds are listed in Table 8.

In the structure of **14**, three copper atoms are 3-fold coordinated and the other three are 4-fold coordinated. The latter are bound to the $MeGa(SPh)_3^-$ fragment, a Me_3P ligand, and two phenylthiolate ligands. Most of the Cu−S bond lengths are typical for the coordination number of the copper atoms, except the 3-fold coordinated atoms Cu5 and Cu6, which have a long bond of ca. 239 pm to S5, and a very short bond of ca. 220 pm to S7 or S8, respectively. This rather large difference is a consequence of the μ_4-bridging mode of S5, weakening the bonds to this atom. Therefore, the angles S4−Cu5−S7 (147°) and S6−Cu6−S8 (146°) are large. The Ga−S bond lengths range from 229.69(7) pm to 233.48(8) pm. The heavy atom framework of **14** contains an approximate mirror plane through Ga1, S1, Cu1, P1, S5, Cu4, and P4.

The selenium compounds **15**−**17** crystallize in trigonal or cubic space groups, and the molecules contain a crystallographic 3-fold axis through C1, Ga1, and Cu4 in each case. As an example, the molecular structure of $[(Me_3P)_3Cu_4MeGa(SePh)_6]$ (**15**) is shown in Figure 10.

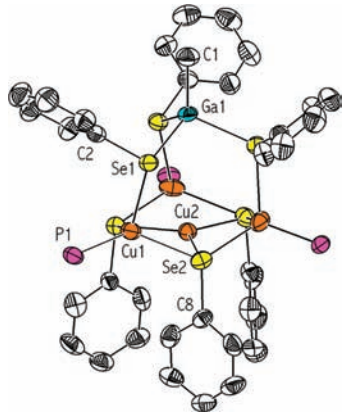

Figure 10. Molecular structure of $[(Me_3P)_3Cu_4MeGa(SePh)_6]$ (**15**). Hydrogen atoms and alkyl groups of phosphine ligands omitted, 50% probability ellipsoids.

The structures of the fragments $MeGa(SePh)_3^-$ and the free ion are very similar, with Ga−Se bond lengths of 243 pm. The copper centered six-membered ring $(R_3P)_3Cu_4(SePh)_3^+$ was also observed as part of the binary copper complex $[(Et_3P)_5(CuSePh)_6]$.[7b] Interestingly, a completely different structure was found for the homologous sulfur compound $[(Et_3P)_5(CuSPh)_6]$, not containing such a copper centered ring.[7b] Obviously, the Cu_3S_3 ring is too small to accommodate a copper atom in its center, causing the different structures. As the main result of the variation of the phosphine ligand in compounds **15**−**17**, the unit cell and the packing of the molecules therein change. Only small differences are observed in the molecular structures: one Cu−Se bond is about 5 pm elongated in **16** and **17**, leading to a larger Cu_3Se_3 ring in **16** or a somewhat larger distance of this ring to the $MeGa(SePh)_3^-$ fragment in **17**.

The homologous tellurium compound **18** (Figure 11) exhibits in principle the same molecular structure as found for **15**−**17**. The main difference is a rotated phenyltellurolate ligand in the $MeGa(TePh)_3^-$ fragment, as was observed for the ionic compound **5**. Again, this rotation breaks the 3-fold symmetry and may be due to crystal packing effects. This complex is probably the first example of a molecular compound containing the elements Cu, Ga, and Te, which was structurally characterized.[18] The Ga−Te bond lengths vary between 262.17(4) and 267.24(4) pm, and are therefore somewhat longer than in the free anion $[MeGa(TePh)_3]^-$ in **5**. The Cu−Te bond lengths range from 260.19(4) to 270.16(5) pm.

Thermolysis. Although it seems clear that the thermolysis of the copper rich complexes **14**−**18** will yield binary copper

dx.doi.org/10.1021/ic300278v | Inorg. Chem. 2012, 51, 6655−6666

Table 8. Crystallographic Data for Compounds $[(Me_3P)_4Cu_6MeGa(SPh)_8]$ (14), $[(R_3P)_3Cu_4MeGa(SePh)_6]$ with R_3P = Me_3P (15), Et_3P (16), $Et_2{}^iPrP$ (17), and $[(Et_3P)_3Cu_4MeGa(TePh)_6]$ (18)

	14·0.375C_5H_{12}	15·1.5CH_3OH·0.5C_5H_{12}	16	17	18
chemical formula	$C_{62.9}H_{83.5}Cu_6GaP_4S_8$	$C_{54.5}H_{72}Cu_4GaO_{1.5}P_3$ Se_6	$C_{55}H_{78}Cu_4GaP_3Se_6$	$C_{58}H_{84}Cu_4GaP_3Se_6$	$C_{55}H_{78}Cu_4GaP_3Te_6$
fw [g mol^{-1}]	1666.08	1647.84	1629.72	1671.80	1921.56
space group	$P2_1/n$ (No. 14)	$P\bar{3}c$ (No. 165)	$P2_13$ (No. 198)	$R3$ (No. 146)	$P2_1/c$ (No. 14)
a [Å]	12.4658(4)	16.3325(7)	18.5472(4)	13.9261(6)	23.2628(8)
b [Å]	25.0048(9)	16.3325(7)	18.5472(4)	13.9261(6)	13.1277(5)
c [Å]	23.5111(7)	27.162(2)	18.5472(4)	29.519(2)	23.5164(9)
α [deg]	90	90	90	90	90
β [deg]	95.505(2)	90	90	90	111.598(3)
γ [deg]	90	120	90	120	90
V [$Å^3$]	7294.7(4)	6274.7(5)	6380.2(2)	4957.8(4)	6677.4(4)
Z	4	4	4	3	4
D_{calcd} [g cm^{-3}]	1.517	1.725	1.697	1.680	1.911
μ [Mo Kα, mm^{-1}]	2.432	5.350	5.259	5.079	4.325
R1 [$I > 2\sigma(I)$]	0.0309	0.0345	0.0240	0.0390	0.0224
wR2 [all data]	0.0800	0.0744	0.0548	0.1069	0.0395

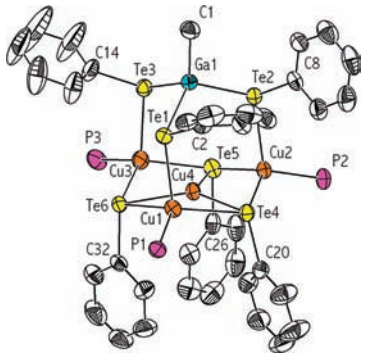

Figure 11. Molecular structure of $[(Et_3P)_3Cu_4MeGa(TePh)_6]$ (18). Hydrogen atoms and alkyl groups of phosphine ligands omitted, 50% probability ellipsoids.

chalcogenides as main component, we tested this for the compounds 15, 17, and 18 (Supporting Information, Figures S27–S29 and S43–S45). The end temperatures extrapolated from the TG curves are below 300 °C in all cases, and the lowest end temperature of 256 °C is observed for the tellurium compound 18. The proportion of $CuGaTe_2$ in the residue is 33.6(3)% in this case, with the rest being binary copper telluride. The end temperatures for the selenium compounds 15 and 17 are somewhat higher, and the proportion of ternary semiconductor is lower.5

5. Tri-*tert*-butylphosphonium Salts. In contrast to the other phosphines R_3P (R = Me, Et, ^{i}Pr), no ternary monomethyl compounds with tri-*tert*-butylphosphine as ligand could be isolated. Attempts to synthesize ^{t}Bu_3P-stabilized copper monomethyl gallium complexes resulted in the protonation of ^{t}Bu_3P. By reaction of 7 with further phenylthiol, colorless crystal blocks of $(^tBu_3PH)[MeGa(SPh)_3]$ (19) were obtained instead of a ternary complex. A similar experiment with $[(^tBu_3P)_3(CuTePh)_4]$[7b] as starting material led to the formation of yellow needles of $(^tBu_3PH)_2[Cu_4(TePh)_6]$ (20). Crystallographic data for the two unexpected products 19 and 20 are summarized in Table 9.

The structure of 19 is shown in Figure 12. This ionic compound consists of a phosphonium cation and the anion $[MeGa(SPh)_3]^-$. Although there are no crystallographic symmetry elements in the ions, both are close to C_3-symmetry.

Table 9. Crystallographic Data for $(^tBu_3PH)[MeGa(SPh)_3]$ (19) and $(^tBu_3PH)_2[Cu_4(TePh)_6]$ (20)

	19	20·C_4H_8O
chemical formula	$C_{31}H_{46}GaPS_3$	$C_{64}H_{94}Cu_4OP_2Te_6$
fw [g mol^{-1}]	615.55	1961.09
space group	$P2_1/n$ (No. 14)	$P2_1/n$ (No. 14)
a [Å]	11.5239(5)	12.1775(5)
b [Å]	25.137(1)	23.224(1)
c [Å]	12.0520(5)	26.157(1)
α [deg]	90	90
β [deg]	113.356(3)	103.179(3)
γ [deg]	90	90
V [$Å^3$]	3205.2(3)	7202.6(5)
Z	4	4
D_{calcd} [g cm^{-3}]	1.276	1.808
μ [Mo Kα, mm^{-1}]	1.122	3.628
R1 [I > 2σ(I)]	0.0348	0.0386
wR2 [all data]	0.0840	0.1241

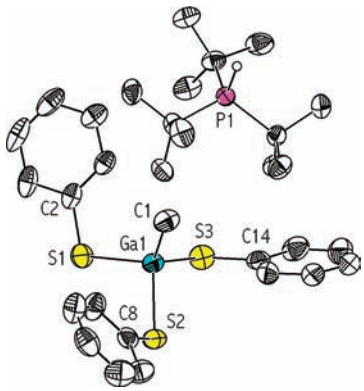

Figure 12. Structure of $(^tBu_3PH)[MeGa(SPh)_3]$ (19). Only the hydrogen atom bound to the phosphorus atom is shown, 50% probability ellipsoids for C, Ga, P, and S atoms.

Bond lengths and angles in the anion are very similar to those found for compound 3.

In 20 two phosphonium cations compensate the charge of the anion $[Cu_4(TePh)_6]^{2-}$ (Figure 13). The homologous anions with E = S and Se have been described already in the literature.[19] The four copper atoms forming a tetrahedron are

dx.doi.org/10.1021/ic300278v | Inorg. Chem. 2012, 51, 6655–6666

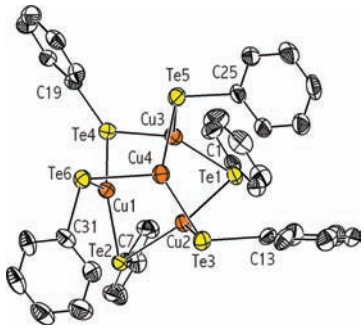

Figure 13. Structure of the anion in $(^tBu_3PH)_2[Cu_4(TePh)_6]$ (**20**), 50% probability ellipsoids.

coordinated in a trigonal planar fashion by six phenyltellurolate ligands. The six tellurium atoms form an octahedron, leading to an adamantane-like structure for the heavy atom framework. The Cu−Te bond lengths range from 254.7(1) to 260.5(1)pm. The Te−Cu−Te angles show values between 105° and 137°; the Cu−Te−Cu angles (64° to 69°) are relatively small.

SUMMARY AND CONCLUSIONS

We isolated a series of 18 different organometallic trialkylphosphine-stabilized copper(I) gallium(III) phenylchalcogenolate complexes, and characterized them by single crystal X-ray crystallography. All these complexes contain one tetrahedrally coordinated gallium atom as part of the fragment $Me_2Ga(EPh)_2^-$ or $MeGa(EPh)_3^-$, in the cases of **1**−**5** as free gallate anions. The copper content and therefore the overall nuclearity of the complexes is mainly influenced by size and amount of the phosphine ligand. A similar observation has been reported for phosphine coordinated cluster compounds.[20] Four different copper containing fragments are observed: the free ion $[(Me_3P)_4Cu]^+$ (in **1**−**5**), the ring fragment $(R_3PCu)_2EPh^+$ with R = Et, ^{i}Pr, ^{t}Bu and E = S, Se (in **6**−**13**), the copper phenylthiolate cage fragment $(Me_3P)_4Cu_6(SPh)_5^+$ (in **14**), and the copper centered six membered rings $(R_3P)_3Cu_4(EPh)_3^+$ with R_3P = Me_3P, Et_3P, $Et_2{}^iPrP$ and E = Se, Te (in **15**−**18**).

The Cu−E bond lengths are very flexible and show the usual dependence on the coordination number of the copper atom. Mean values (in the order E = S, Se, and Te) for 3-fold coordination are 228, 242, and 263 pm. The respective values for 4-fold coordination are 240, 254, and 266 pm. These mean values are nearly the same as in the related binary complexes $[(R_3P)_m(CuEPh)_n]$,[7b] and maximum deviations are 2 pm. As found for these binary complexes, the dependence of the Cu−P bond lengths on the coordination number is less pronounced, and mean values are 223 and 226 pm for 3-fold and 4-fold coordination, respectively. The Ga−E bond lengths are less flexible and depend mainly on the number of methyl groups bound to the gallium atom, with shorter bonds for monomethyl compounds. The distribution of Cu−E and Ga−E bond lengths is shown in Figure 14. Interestingly, the Ga−E bonds show the tendency to be shorter in the ternary dimethyl gallium complexes compared to the binary dimethyl gallium phenylchalcogenolates $[(Me_2GaEPh)_n]$. Values found for the binary compounds are 236−243 pm for E = S, 251−253 pm for E = Se, and 272−276 pm for E = Te.[8b] This shows that the CuEPh moiety is a stronger donor to the gallium atom than the GaEPh moiety, which means that the ternary complexes are energetically more stable compared to the binary compounds.

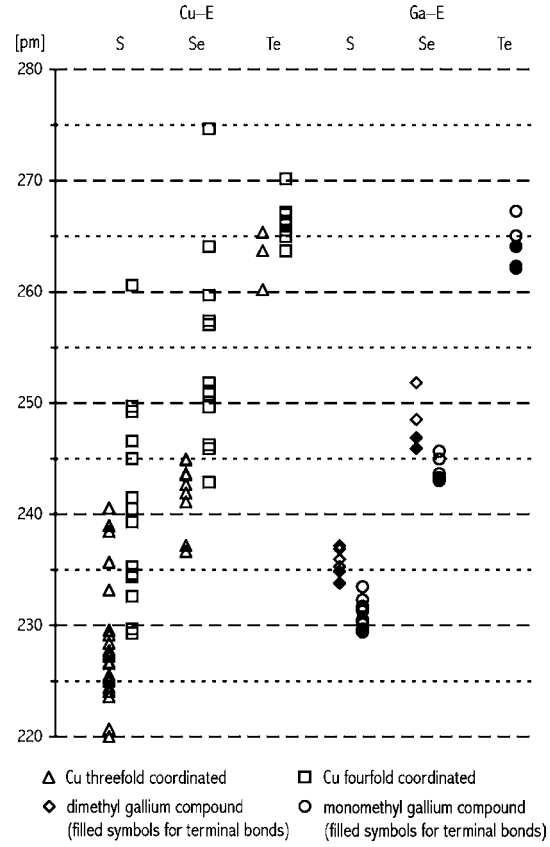

Figure 14. Cu−E and Ga−E (E = S, Se, Te) bond lengths in complexes **1**−**18**.

The thermolysis process of sulfur-containing complexes usually starts with the release of the phosphine ligands and ends with the release of Me_3Ga and SPh_2. This is in contrast to results on other single-source precursors, where the chalcogenide moiety is released first, followed by the phosphine ligand,[6c] but this may be simply an effect of relative volatility. For the heavier chalcogens we observed a tendency for lower end temperatures extrapolated from TG curves, and more complicated mechanisms. The thermolysis leads to the respective semiconductor $CuGaE_2$ in all cases. The release of Me_3Ga during the thermolysis process and the excess of copper in complexes **6**−**18** results in the formation of binary copper chalcogenides as additional phases. This is not necessarily a disadvantage, as indicated in the Introduction, since it is well-known that a copper rich deposition of thin films results in improved film crystallinity.[2,3] From investigations on thin film deposition with the single source precursor $[(Ph_3P)_2CuIn(SEt)_4]$, it was concluded that "the grain size was small due to the absence of a quasi-liquid Cu binary phase. Further development is necessary to grow films with higher Cu concentration...".[6h] Therefore, at least the precursors which yield the ternary semiconductor as main component, such as **3**−**5**, may be promising candidates for thin film deposition experiments. Furthermore, we could show that mixing of different types of chalcogen atoms is possible on the molecular level. Reaction of the sulfur compound **6** with $Me_3SiSePh$ and MeOH yields the mixed sulfur−selenium compound **13** that can be thermolyzed to the quaternary semiconductor of the approximate formula $CuGaS_{1.5}Se_{0.5}$.

dx.doi.org/10.1021/ic300278v | Inorg. Chem. 2012, 51, 6655−6666

■ ASSOCIATED CONTENT

Supporting Information

Experimental and computational details; NMR spectra corresponding to ref 14; ORTEP plots of compounds **2**, **3**, **10**, **12**, **16**, and **17**; tables of selected bond lengths and angles; TG curves; *in situ* X-ray powder diffraction patterns of the thermolysis of **12**; Rietveld refinement plots; crystallographic information in CIF format. This material is available free of charge via the Internet at http://pubs.acs.org.

■ AUTHOR INFORMATION

Corresponding Author

*E-mail: krautscheid@rz.uni-leipzig.de.

Notes

The authors declare no competing financial interest.

■ ACKNOWLEDGMENTS

Financial support by the University of Leipzig (PbF-1) is gratefully acknowledged. We thank URZ Leipzig for computational resources.

■ DEDICATION

Dedicated to Professor Dieter Fenske on occasion of his 70th birthday.

■ REFERENCES

(1) (a) Rockett, A. A. *Curr. Opin. Solid State Mater. Sci.* **2010**, *14*, 143−148. (b) Kaneshiro, J.; Gaillard, N.; Rocheleau, R.; Miller, E. *Sol. Energy Mater. Sol. Cells* **2010**, *94*, 12−16. (c) Niki, S.; Contreras, M.; Repins, I.; Powalla, M.; Kushiya, K.; Ishizuka, S.; Matsubara, K. *Prog. Photovoltaics* **2010**, *18*, 453−466. (d) Avrutin, V.; Izyumskaya, N.; Morkoç, H. *Superlattices Microstruct.* **2011**, *49*, 337−364. (e) Klenk, R.; Klaer, J.; Köble, C.; Mainz, R.; Merdes, S.; Rodriguez-Alvarez, H.; Scheer, R.; Schock, H.-W. *Sol. Energy Mater. Sol. Cells* **2011**, *95*, 1441−1445.

(2) Klenk, R.; Walter, T.; Schock, H.-W.; Cahen, D. *Adv. Mater.* **1993**, *5*, 114−119.

(3) Klenk, R.; Klaer, J.; Scheer, R.; Lux-Steiner, M. C.; Luck, I.; Meyer, M.; Rühle, U. *Thin Solid Films* **2005**, *480*−*481*, 509−514.

(4) (a) Vittal, J. J.; Ng, M. T. *Acc. Chem. Res.* **2006**, *39*, 869−877. (b) Fan, D.; Afzaal, M.; Mallik, M. A.; Nguyen, C. Q.; O'Brien, P.; Thomas, P. J. *Coord. Chem. Rev.* **2007**, *251*, 1878−1888. (c) Mallik, M. A.; Afzaal, M.; O'Brien, P. *Chem. Rev.* **2010**, *110*, 4417−4446. (d) Afzaal, M.; Mallik, M. A.; O'Brien, P. *J. Mater. Chem.* **2010**, *20*, 4031−4040.

(5) (a) Hirpo, W.; Dhingra, S.; Kanatzidis, M. G. *J. Chem. Soc., Chem. Commun.* **1992**, 557−559. (b) Eichhöfer, A.; Fenske, D. *J. Chem. Soc., Dalton Trans.* **2000**, 941−944. (c) Tran, D. T. T.; Beltran, L. M. C.; Kowalchuk, C. M.; Trefiak, N. R.; Taylor, N. J.; Corrigan, J. F. *Inorg. Chem.* **2002**, *41*, 5693−5698. (d) Olkowska-Oetzel, J.; Fenske, D.; Scheer, P.; Eichhöfer, A. *Z. Anorg. Allg. Chem.* **2003**, *629*, 415−420. (e) Eichhöfer, A.; Fenske, D.; Olkowska-Oetzel, J. *Z. Anorg. Allg. Chem.* **2004**, *630*, 247−251. (f) Ahlrichs, R.; Crawford, N. R. M.; Eichhöfer, A.; Fenske, D.; Hampe, O.; Kappes, M. M.; Olkowska-Oetzel, J. *Eur. J. Inorg. Chem.* **2006**, 345−350. (g) Williams, M.; Okasha, R. M.; Nairn, J.; Twamley, B.; Afifi, T. H.; Shapiro, P. J. *Chem. Commun.* **2007**, 3177−3179. (h) Wang, L.; Wu, T.; Zuo, F.; Zhao, X.; Bu, X.; Wu, J.; Feng, P. *J. Am. Chem. Soc.* **2010**, *132*, 3283−3285. (i) Wu, T.; Wang, L.; Bu, X.; Chau, V.; Feng, P. *J. Am. Chem. Soc.* **2010**, *132*, 10823−10831. (j) Xiong, W.-W.; Li, J.-R.; Hu, B.; Tan, B.; Li, R.-F.; Huang, X.-Y. *Chem. Sci.* **2012**, *3*, 1200−1204.

(6) (a) Hirpo, W.; Dhingra, S.; Sutorik, A. C.; Kanatzidis, M. G. *J. Am. Chem. Soc.* **1993**, *115*, 1597−1599. (b) Hollingsworth, J. A.; Hepp, A. F.; Buhro, W. E. *Chem. Vap. Deposition* **1999**, *5*, 105−108. (c) Banger, K. K.; Hollingsworth, J. A.; Harris, J. D.; Cowen, J.; Buhro, W. E.; Hepp, A. F. *Appl. Organomet. Chem.* **2002**, *16*, 617−627. (d) Banger, K. K.; Jin, M. H.-C.; Harris, J. D.; Fanwick, P. E.; Hepp, A. F. *Inorg. Chem.* **2003**, *42*, 7713−7715. (e) Hollingsworth, J. A.; Banger, K. K.; Jin, M. H.-C.; Harris, J. D.; Cowen, J. E.; Bohannan, E. W.; Switzer, J. A.; Buhro, W. E.; Hepp, A. F. *Thin Solid Films* **2003**, *431*−*432*, 63−67. (f) Harris, J. D.; Banger, K. K.; Scheiman, D. A.; Smith, M. A.; Jin, M. H.-C.; Hepp, A. F. *Mater. Sci. Eng.* **2003**, *B98*, 150−155. (g) Deivaraj, T. C.; Park, J.-H.; Afzaal, M.; O'Brien, P.; Vittal, J. J. *Chem. Mater.* **2003**, *15*, 2383−2391. (h) Jin, M. H.-C.; Banger, K. K.; Harris, J. D.; Hepp, A. F. *Mater. Sci. Eng.* **2005**, *B116*, 395−401. (i) Banger, K. K.; Hepp, A. F.; Harris, J. D.; Jin, M. H.-C.; Castro, S. L. U.S. Patent US 6992202 B1, 2006. (j) Ng, M. T.; Vittal, J. J. *Inorg. Chem.* **2006**, *45*, 10147−10154. (k) Adams, R. D.; Captain, B.; Zhang, Q.-F. *Z. Anorg. Allg. Chem.* **2007**, *633*, 2187−2190. (l) Margulieux, K. R.; Sun, C.; Zakharov, L. N.; Holland, A. W.; Pak, J. J. *Inorg. Chem.* **2010**, *49*, 3959−3961. (m) Sun, C.; Westover, R. D.; Margulieux, K. R.; Zakharov, L. N.; Holland, A. W.; Pak, J. J. *Inorg. Chem.* **2010**, *49*, 4756−4758. (n) Han, Y.-G.; Xu, C.; Duan, T.; Zhang, Q.-F. *Inorg. Chim. Acta* **2011**, *365*, 414−418.

(7) (a) DeGroot, M. W.; Cockburn, M. W.; Workentin, M. S.; Corrigan, J. F. *Inorg. Chem.* **2001**, *40*, 4678−4685. (b) Kluge, O.; Grummt, K.; Biedermann, R.; Krautscheid, H. *Inorg. Chem.* **2011**, *50*, 4742−4752.

(8) (a) Coates, G. E.; Hayter, R. G. *J. Chem. Soc.* **1953**, 2519−2524. (b) Kluge, O.; Gerber, S.; Krautscheid, H. *Z. Anorg. Allg. Chem.* **2011**, *637*, 1909−1921.

(9) Haaland, A. *Angew. Chem., Int. Ed. Engl.* **1989**, *28*, 992−1007.

(10) Maelia, L. E.; Koch, S. A. *Inorg. Chem.* **1986**, *25*, 1896−1904.

(11) Han, Y.-G.; Xu, C.; Duan, T.; Zhang, Q.-F.; Leung, W.-H. *J. Mol. Struct.* **2009**, 15−18.

(12) Dean, P. M.; Pringle, J. M.; MacFarlane, D. R. *Phys. Chem. Chem. Phys.* **2010**, *12*, 9114−9153.

(13) Janosi, A. *Acta Crystallogr.* **1964**, *17*, 311−312.

(14) For $Me_3Ga{-}PMe_3$, ^1H NMR: δ = −0.11 ppm (s, 9H), 0.55 ppm (d, $^2J_{HP}$ = 6 Hz, 9H). $^{13}C\{^1H\}$ NMR: δ = −7.8 ppm (s), 10.0 ppm (d, J_{CP} = 12 Hz). $^{31}P\{^1H\}$ NMR: δ = −44.5 ppm (s). For MeSePh, ^1H NMR: δ = 1.89 ppm (s, 3H), 6.95 ppm (m, 3H), 7.25 ppm (d, $^3J_{HH}$ = 7 Hz, 2H). $^{13}C\{^1H\}$ NMR: δ = 6.6 ppm (s + d, J_{CSe} = 64 Hz), 126.1 ppm (s), 129.2 ppm (s), 130.5 ppm (s), 132.5 ppm (s). $^{77}Se\{^1H\}$ NMR: δ = 202 ppm (s). In accordance with the following: McFarlane, W.; Wood, R. J. *J. Chem. Soc., Dalton Trans.* **1972**, 1397−1402. O'Brien, D. H.; Dereu, N.; Huang, C.-K.; Irgolic, K. J.; Knapp, F. F. *Organometallics* **1983**, *2*, 305−307. For Me_3PSe, ^1H NMR: δ = 1.20 ppm (d, $^2J_{HP}$ = 13 Hz). $^{13}C\{^1H\}$ NMR: δ = 22.6 ppm (d, J_{CP} = 48 Hz). $^{31}P\{^1H\}$ NMR: δ = 6.1 ppm (s + d; J_{PSe} = 714 Hz). In accordance with the following: McFarlane, W.; Rycroft, D. S. *J. Chem. Soc., Chem. Commun.* **1972**, 902−903. McFarlane, W.; Rycroft, D. S. *J. Chem. Soc., Dalton Trans.* **1973**, 2162−2166. Kuhn, N.; Schumann, H. *J. Organomet. Chem.* **1986**, *304*, 181−193. For $SePh_2$, ^1H NMR: δ = 6.92 (m, 6H), 7.40 (m, 4H). $^{13}C\{^1H\}$ NMR: δ = 127.3 (s), 129.5 (s), 131.6 (s), 133.2 (s + d, $^2J_{CSe}$ = 12 Hz). $^{77}Se\{^1H\}$ NMR: δ = 416 ppm (s). In accordance with the following: Wrackmeyer, B.; Klimkina, E. V.; Milius, W. *Z. Anorg. Allg. Chem.* **2006**, *632*, 2331−2340. Klapötke, T. M.; Krumm, B.; Scherr, M. *Inorg. Chem.* **2008**, *47*, 4712−4722 . For details of NMR measurement conditions and complete spectra, see Supporting Information (Figures S1−S8).

(15) Burns, J. A.; Pennington, W. T.; Robinson, G. H. *Organometallics* **1995**, *14*, 1533−1535.

(16) Skomorokhov, A. N.; Trots, D. M.; Knapp, M.; Bickulova, N. N.; Fuess, H. *J. Alloys Compd.* **2006**, *421*, 64−71.

(17) (a) Cremer, D.; Pople, J. A. *J. Am. Chem. Soc.* **1975**, *97*, 1354−1358. (b) Boeyens, J. C. A. *J. Cryst. Mol. Struct.* **1978**, *8*, 317−320 . Atom sequence Ga1−E1−Cu1−E3−Cu2−E2. Values for **6**: θ = 88.26(2)°, ϕ = 331.71(2)°. For **7**: θ = 98.00(4)°, ϕ = 278.33(3)°. For **8**: θ = 90.15(2)°, ϕ = 310.05(3)°.

(18) Recent CCDC and ICSD search shows no entries for molecular compounds containing Cu, Ga, and Te.

(19) (a) Coucouvanis, D.; Murphy, C. N.; Kanodia, S. K. *Inorg. Chem.* **1980**, *19*, 2993−2998. (b) Baumgartner, M.; Bensch, W.; Hug,

P.; Dubler, E. *Inorg. Chim. Acta* **1987**, *136*, 139−147. (c) Jin, X.; Tang, K.; Long, Y.; Tang, Y. *Acta Crystallogr.* **1999**, *C55*, 1799−1800.
(20) (a) Fenske, D.; Krautscheid, H.; Müller, M. *Angew. Chem.* **1992**, *104*, 309−312. (b) Fenske, D. In *Clusters and Colloids*; Schmid, G., Ed.; VCH: Weinheim, 1994; pp 212−297.